Journal of Chemical and Petroleum Engineering (JChPE)

Print ISSN: 2423-673X Online ISSN: 2423-6721

2D-CFD Analysis of Diffusers used to Discharge Brine into Water Bodies

Iman Moshiri-Tabrizi, Mohammad-Hossein Sarrafzadeh*, Rahmat Sotudeh-Gharebagh**

1. UNESCO Chair on Water Reuse, College of Engineering, University of Tehran, Tehran, Iran. E-mail: iman.moshiri@ut.ac.ir
2. UNESCO Chair on Water Reuse, College of Engineering, University of Tehran, Tehran, Iran. E-mail: sarrafzdh@ut.ac.ir
3. School of Chemical Engineering, College of Engineering, University of Tehran, Tehran, Iran. E-mail: sotudeh@ut.ac.ir

ARTICLE INFO

Article History:
Received: 28 May 2021
Revised: 08 July 2023
Accepted: 10 July 2023

Article type: Research

Keywords:
Computational Fluid-Dynamics,
Dense Discharge,
Integral Models,
Marine Environment,
Submerged Diffusers

ABSTRACT

Inclined submerged diffusers that are used to dilute hypersaline and highly contaminated brine, discharged from desalination plants, in receiving marine waters are commonly modeled via semi-empirical, integral, and 3D Computational Fluid Dynamic (CFD) models. The first two models are computationally simple and efficient, but not enough accurate in many cases, and 3D-CFD models which show good agreement with experimental data are time-consuming. To avoid computational costs of 3D models and to present a more precise model than simple ones, a modified 2D-CFD model for stagnant and dynamic ambient is suggested in this study. The results showed that the proposed model can predict the jet behavior in both ambients more accurately than integral models and in shorter computing time than 3D models. The results of this study can be used in order to design environmentally friendly discharge systems by engineers and practitioners for brine or pollutant dilution in the receiving marine waters.

Introduction

In recent years, the water shortage has become a serious and ongoing challenge in most countries around the world due to various reasons; i.e. population growths, industrial and agricultural developments, and limited freshwater resources [1,2]. Therefore, comprehensive technologies are needed in order to deal with these challenges. Among the existing technologies, membrane-based desalination technologies are received more attentions. These are classified as reverse osmosis (RO), nano-filtration (NF), electrodialysis (ED), membrane distillation (MD), forward osmosis (FO), electrodialysis reversal (EDR), electrodeionization (EDI), and their combination as hybrid technologies. Although RO is the leading and most common technology accounted for ~70% of desalination plants worldwide, one must properly deal with effluent generated in these plants which is the major drawback of this technology [3-7].

* Corresponding Authors: M. Sarrafzadeh, R. Sotudeh-Gharebagh (E-mail address: sarrafzdh@ut.ac.ir, sotudeh@ut.ac.ir)

Journal of Chemical and Petroleum Engineering, 2023, 57(2): 303- 319.
Publisher: University of Tehran, College of Engineering *DOI: 10.22059/jchpe.2023.321150.1347*

The RO technology, as well as FO and MD, has the highest ratio of effluents to intake seawater with approximately 60%, whereas the equivalent figures for NF, ED and EDI are 31%, 14%, and 10%, respectively [8]. The hypersaline effluent of RO plants, referred to as brine, contains high concentrations of various chemicals such as pretreatment biocides coagulants, antiscalants, antifoaming agents, and heavy metals (e.g., copper) that are used or generated during the plant operation. In addition, maybe as a result of insufficient treatment in wastewater treatment plants, unremoved emerging pollutants, like trace organic chemicals (e.g., personal care products), effluent organic matter (e.g., soluble microbial products), and pathogens, are discharged to surface waters which are the feed source of RO desalination plants. Inevitably, brine suffers from these emerging pollutants as well [9,10]. Inappropriate disposal of the brine would lead to an increase in local salinity and pollutants' concentration in the receiving area causing adverse effects on vulnerable benthic infaunal communities and seagrasses creating severe environmental problems on marine ecosystems [3,11,12]. Therefore, appropriate disposal methods should be designed and put in place to handle the effluent.

The commonly used disposal methods in seawater desalination plants, which were reported in the open literature, are surface-water and sewer discharge, deep-well injection, evaporation ponds, and land disposal. The surface-water discharge method, which accounts for more than 90% of disposal methods, can be regarded on three distinct configurations as surface, over surface, and submerged discharge configurations [13,14]. Among these configurations, the submerged discharge with single-, multi-port, and rosette-shaped diffusers is more commonly used, particularly first two diffusers, since they effectively promote enhanced mixing of the salty plume in the receiving areas [3,15,13,16].

Single- and multi-port diffusers can handle brine at a variety of discharge angles to the horizontal axis ranged from 0° to 90° forming horizontal, inclined, and vertical jets, respectively. There are a significant number of studies in the literature aiming to find the optimal discharge angle. Zeitoun et al. reported that an angle of 60° can provide the longest jet trajectory and the maximum achievable dilution for the discharged brine [17]. This was accepted as the *de facto* standard for design before Abessi and Roberts proved it thorough experiments with 3DLIF* [18,19].

Design and operation of submerged disposal devices of dense effluent is not only restricted to jet characteristics, i.e. the optimum discharge angle [15], but also dilution parameters of brine-water mixture at the receiving area should be taken into consideration. These parameters are physical properties of the brine and receiving water, diffuser configurations and flow pattern, discharge velocity, ambient conditions, etc. Experimental and numerical techniques should be applied to study the effect of these parameters accurately in order to help the scientists and designers.

Experimental work with submerged discharge devices is rather tedious, expensive, and time-consuming, therefore, simulation tools should be applied to reduce the experimental costs and time. Numerical modeling and simulation can be used to predict the behavior of submerged discharge of the brine into the receiving area. Three main types of numerical models were reported in the literature for brine discharge modeling. First, semi-empirical models based on dimensional analysis i.e. CORMIX1, applicable to submerged and emerged single port jets, and CORMIX2 which models submerged multiport jets, sub-models from CORMIX software. Second, models based on integration of governing equations (also known as integral models) i.e. CORJET from CORMIX software, JETLAG from VISJET software, and UM3 from VISUAL PLUMES. Third, models based on CFD, which are widely used in pollutants

* Three-Dimensional Laser-Induced Fluorescence (3DLIF)

modeling; i.e. water and air pollution dispersion, effluent discharge and in submerged discharge systems [20-26].

The predictions provided by semi-empirical models are limited to conditions where these models were developed. While integral models predict the characteristics of dense inclined jets more accurately compared to semi-empirical models, their accuracy in predicting the experimental data is still not widely acceptable, especially in a dynamic ambient [27]. On the other hand, CFD uses more justified hypotheses and comprehensive governing equations, and it enjoys strong solvers in dealing with equations which could lead to more reliable and sound results. However, although the advancement of computing systems as well as a significant reduction in data storage costs have made using these models more demanding, 3D CFD models are still computationally much more expensive as compared with semi-empirical and integral models, therefore in some cases 2D models are much more preferable if dimensionality reduction of 3D models is made wisely. Based on the literature, in the last 15 years, several studies have utilized CFD to simulate the dilution pattern and geometrical characteristics of inclined dense jets. Table 1 summarizes these studies for submerged inclined jets.

The Table reveals three meaningful points. First, the deviations between models and experimental data were mostly attributed to the type of turbulence model and the quality of meshes used. Second, most of the numerical studies on submerged diffusers, have only focused on stagnant ambient and there is no study aimed at comparing computational fluid dynamics (CFD) with integral models in both stagnant and dynamic environments. Third, to the best of the authors' knowledge, numerical studies using CFD have proposed a 3D model which is significantly time consuming. On the other hand, the 2D model is expected to be more accurate and efficient as compared with integral models. Therefore, the main objective of this study is to evaluate the applicability of the 2D model to analyze submerged discharge systems in both stagnant and dynamic ambient and comparing the results with integral model

Table 1. A Summary of Recent Studies on CFD Modeling of Submerged Inclined Jets

Tool	Angle (°)	Turbulence Closure	Ambient	Remark	Ref.
ANSYS CFX	45 60 70 80 90	SST† *k-ω*	Stagnant	• First Study Applying CFD • Underestimate Maximum Rise Height • Underestimate Impact Point Location	[28]
	60	standard *k-ε*		• Overpredict Centerline Concentration	[29]
Fluidity	60	Standard *k-ε*, Smagorinsky LES‡		• Underestimate Dilution Pattern • Underpredict with Standard *k-ε*	[30]
Open FOAM®	30 45	Five Models§		• Comparing Accuracy of Models	[31]
	45 60			• Underestimate Impact Dilution • Insufficient Grid Resolution	[32]
	45	LES		• Deviations from Experimental Data • Low Mesh Quality	[33]
	45	Realizable *k-ε*		• Thermal-Saline Negatively Buoyant Jets • Deviations for Plume-Like Zone Data	[34]
	60	Standard *k-ε*, RNG** *k-ε*		• moderately spaced ports diffuser • Significant errors with standard *k-ε*	[15]
		SST *k-ω*	Dynamic		[35]

† Shear Stress Transport (SST)

‡ Large Eddy Simulation (LES)

§ Including 1-RNG k-ε, 2-realizable k-ε, 3-nonlinear k-ε, 4-Launder Reece Rodi (LLR),5- Launder–Gibson

** Re-Normalization Group (RNG)

FLUENT	90	Standard *k-ε*	• No Comparison with Experimental Data	[36]

CFD Modeling

This section provides the analysis of inclined jets and CFD modeling including the governing equations and model setup.

Inclined Jets Behavior

Inclined jets are frequently used to discharge effluents like brine which form a negatively buoyant jet since they are generally more dense than the receiving ambient [37]. The interaction of momentum inserted by inclined jet on this ambient and existing negative buoyancy force dictates the hydrodynamic pattern of the jet. Fig. 1 illustrates the key attributes of an inclined jet.

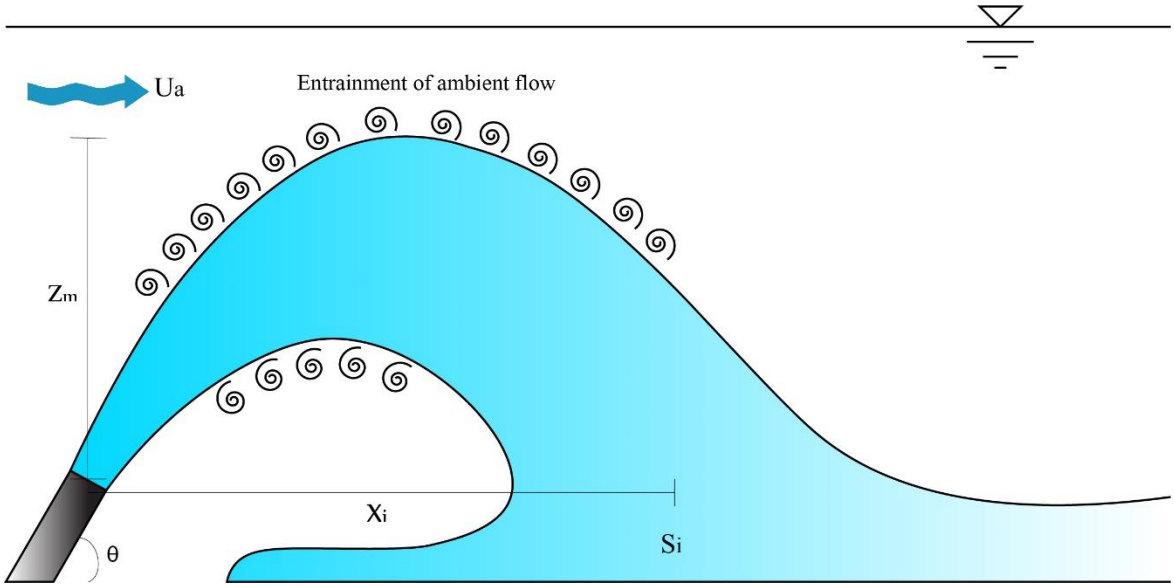

Fig. 1. Schematic of a nozzle and the inclined jet

As the jet with a diffuser diameter of *d* leaves the nozzle with the angle of θ, fixed at 60° in this study, it soon starts ascending to an equilibrium point due to its high discharge velocity and initial momentum. As the jet engulfs the receiving water due to significant pressure difference and turbulent velocity shear, a highly turbulence mixing zone is formed. This allows the jet to be diluted with the receiving water leading to a high decrease in the salinity and pollutants' level.

The equilibrium point, in which the negative buoyancy of jet equates the vertical momentum component, is called the maximum rise height (Z_m). From this point, the jet slightly moves downward as a result of buoyancy forces and the discharge flow bounce back to the bottom boundary at the impact point and after this point, a spreading layer and a gravity current can be seen [38]. It is important to mention that at the impact point, the horizontal distance from the discharge point (X_i), the impact point density (ρ_i), and dilution (S_i) parameters can be measured.

At stagnant ambient, these parameters can be obtained by following expressions with the Boussinesq assumption ($(\rho_0 - \rho_a) \ll \rho_a$), in which ρ_0 is the jet density and ρ_a is the receiving ambient density, and considering the fully turbulent flow and fixed discharge angle [38,39].

$$\frac{Z_m}{dF}, \frac{X_i}{dF}, \frac{S_i}{F} = constant \quad (1)$$

where F is Froude number ($F = {U_0}/{\sqrt{g_0' d}}$), $g_0' = g(\rho_0 - \rho_a)/\rho_a$ is the modified gravitational acceleration at the source, g is the gravitational acceleration, U_0 is the jet velocity.

At a dynamic environment, a variety of orientations can be assumed for ambient flow, ranging from co-flow, in the same direction as the jet, to counter-flow, in the opposite direction. It is worthy to mention that the dilution decreases gradually from co- to counter-flow [40]. The reason for this change is that, in the worst case, a counter-flow current can cause the jet to fall back on itself, and consequently the dilution decreases since this limits the ambient water entrainment [13]. Therefore, assuming a co-flow relative to discharge propagation seems more desirable as it provides a higher dilution rate compared with the counter-flow. In this case, the following expressions can be applied to maximum rise height, impact point location, and impact dilution [35]:

$$\frac{Z_m}{dF}, \frac{X_i}{dF}, \frac{S_i}{F} = f(U_r F) \quad (2)$$

$$U_r = U_a/U_0 \quad (3)$$

where U_r is the ratio of ambient velocity (U_a) to the velocity of effluent on the tip of the nozzle (U_0).

CFD Analysis

This section introduces the governing equations as well as the details of CFD. Multiport diffusers are also useful for brine disposal; however, their behavior is like single jet diffusers [41,42] if the ports are properly spaced. Such spacing would create more dilution and prevent the jets from being merged. Moreover, the simplicity of single jet behavior in dynamic environment analysis would also allow us to model the jet in a small 2D domain which is computationally less expensive than 3D simulations and can reduce computation time significantly. Therefore, in this study, a single jet diffuser is modeled in a 2D domain.

Governing Equations

There are two main fluid phases in the system, i.e., the brine and receiving water. Therefore, it is necessary to apply a two-phase model to predict the interpenetration of these phases moving at two different velocities. In this study, the Mixture model [43] was adopted. The continuity equation for the mixture is:

$$\frac{\partial \rho_m}{\partial t} + \nabla.(\rho_m \vec{u}_m) = 0 \quad (4)$$

where ρ_m is the mixture density:

$$\rho_m = \sum_{i=1}^{n} \alpha_i \rho_i \quad (5)$$

where ρ_i is the density of phase i, α_i is the volume fraction of phase i, u_m is the mass-averaged velocity as:

$$\vec{u}_m = \frac{1}{\rho_m}\sum_{i=1}^{n}\alpha_i\rho_i\vec{u}_i \tag{6}$$

where u_i is the velocity of phase i. The momentum equation for the mixture is:

$$\frac{\partial}{\partial t}\rho_m\vec{u}_m + \nabla.(\rho_m\vec{u}_m\vec{u}_m) = -\nabla p + \nabla.[\mu_m(\nabla\vec{u}_m + \nabla\vec{u}_m^T)] + \nabla.(\sum_{i=1}^{n}\alpha_i\rho_i\vec{u}_{dr,i}\vec{u}_{dr,i}) + \rho_m g + F_b \tag{7}$$

where p is pressure, $\vec{u}_m^T$ is the transpose of mixture velocity matrix, n is the number of phases, F_b is a body force, μ_m is the viscosity of the mixture:

$$\mu_m = \sum_{i=1}^{n}\alpha_i\mu_i \tag{8}$$

and $u_{dr,i}$ is the drift velocity for the secondary phase:

$$\vec{u}_{dr,i} = \vec{u}_i - \vec{u}_m \tag{9}$$

The drift velocity leads to a drag force between phases [44]. For the two-fluid flow, three drag models are considered as Schiller and Naumann [45], Morsi and Alexander [46], and symmetric models. Table 2 compares these drag models. It is notable that unlike their similar equations, the symmetric and the Schiller and Naumann models have different expressions for momentum exchange coefficients and particle relaxation time [47].

Table 2. Comparison of Drag Models in Fluid-Fluid Flows

Model	Drag Coefficient	Remark
Schiller and Naumann	$C_D = \begin{cases} 24(1+0.15Re^{0.687})/Re & Re \le 1000 \\ 0.44 & Re > 1000 \end{cases}$	General two-phase flow
Morsi and Alexander	$C_D = a_1 + \frac{a_2}{Re} + \frac{a_3}{Re^2}\ ;\ a_1, a_2, a_3 = f(Re)$	Most complete, less stable
Symmetric	$C_D = \begin{cases} 24(1+0.15Re^{0.687})/Re & Re \le 1000 \\ 0.44 & Re > 1000 \end{cases}$	Transition to dispersed phase

As it is clear from Table 2, the symmetric model cannot be used in this study. In addition, although Morsi and Alexander model is defined over a wide range of Reynolds numbers, it is less stable compared to other models [47]. Therefore, Schiller and Naumann model seems a more suitable choice for this study. The drag function (f_{drag}) and drag coefficient (C_D) of Schiller and Naumann drag model is:

$$f_{drag} = \frac{C_D Re}{24} \tag{10}$$

$$C_D = \begin{cases} 24(1+0.15Re^{0.687})/Re & Re \le 1000 \\ 0.44 & Re > 1000 \end{cases} \tag{11}$$

Along with a proper drag model, choosing an accurate turbulence scheme is of great importance due to its significant role in producing accurate and reliable results. Some studies [28,5,35,48] have used the SST k-ω turbulence scheme successfully. This scheme provides a combination of the k-ε and k-ω turbulence models for boosting the accuracy of the model in wall-bounded flows [35]. This turbulence model was also compared with LES, as one of the common and well-studied models, by Baum et al. [5] and they have concluded that the SST k-ω model is computationally more efficient.

In this study, the SST *k*-ω turbulence scheme is used for RANS[††] equations. The turbulence kinetic energy, *k*, and the specific dissipation rate, ω, are obtained from the followings:

$$\frac{\partial}{\partial t}(\rho_m k) + \nabla.(\rho_m k \vec{u}_m) = \nabla.\left(\Gamma_{k,m}\nabla k\right) + \tilde{G}_{k,m} - Y_{k,m} \quad (12)$$

$$\frac{\partial}{\partial t}(\rho_m \omega) + \nabla.(\rho_m \omega \vec{u}_m) = \nabla.\left(\Gamma_{\omega,m}\nabla \omega\right) + G_{\omega,m} - Y_{\omega,m} + D_{\omega,m} \quad (13)$$

where $\tilde{G}_{k,m}$ is generation of turbulence kinetic energy due to mean velocity gradients, $G_{\omega,m}$ is generation of ω, $\Gamma_{k,m}$ is the term for the effective diffusivity of *k*, $\Gamma_{\omega,m}$ is the term for the effective diffusivity of ω, $Y_{k,m}$ represents the dissipation of *k* due to turbulence, $Y_{\omega,m}$ represents the dissipation of ω due to turbulence, $D_{\omega,m}$ is the cross-diffusion term. All of these terms are calculated from the expressions and model coefficients reported by Menter [49].

Model Setup

In this study, details of the input data and computational domain were adopted from the study conducted by Palomar et al. [27]. Table 3 shows the simulation parameters for both stagnant and dynamic environments used in this study. A 2D model based on the finite volume method and SIMPLE[‡‡] scheme [50] is used for pressure-velocity coupling to solve the governing equations. The model is modified in order to include dilution effect seen in 3D models. The following equations are adapted for this purpose [47];

$$\dot{m}_{ij} = \max\left[0, \lambda_{ij}\right] - \max[0, -\lambda_{ij}] \quad (14)$$

$$\lambda_{ij} = \dot{r}\alpha_i\rho_i \quad (15)$$

where $\dot{m}_{ij}$ is a positive mass flow rate per unit volume from phase *i* to phase *j*, λ_{ij} is the convective mass transfer coefficient, $\dot{r}$ is a constant rate of liquid droplets shrinking.

To discretize the simulation area, structured meshes are mostly utilized with partial refinements near the domain and jet inlet as well as the bottom boundary. Fig. 2 shows mesh grids and boundary conditions of the model. The mesh sensitivity analysis is also performed to reach a satisfactory grid.

Table 3. Simulation Input Parameters for Stagnant and Dynamic Ambient [27]

Parameter	**ρ_0 (kg/m^3)**	**ρ_a (kg/m^3)**	***D* (m)**	***F***	***U*$_0$ (m/s)**	***U*$_r$*F***
Stagnant ambient	1050	1026	0.20	10,20,30,40	2.1, 4.2, 6.3, 8.4	-
Dynamic ambient	1050	1026	0.18	20	4	0.3, 0.75, 1.25, 1.5, 1.87

[††] Reynolds Average Navier-Stokes (RANS)

[‡‡] Semi-implicit method for pressure-linked equations (SIMPLE)

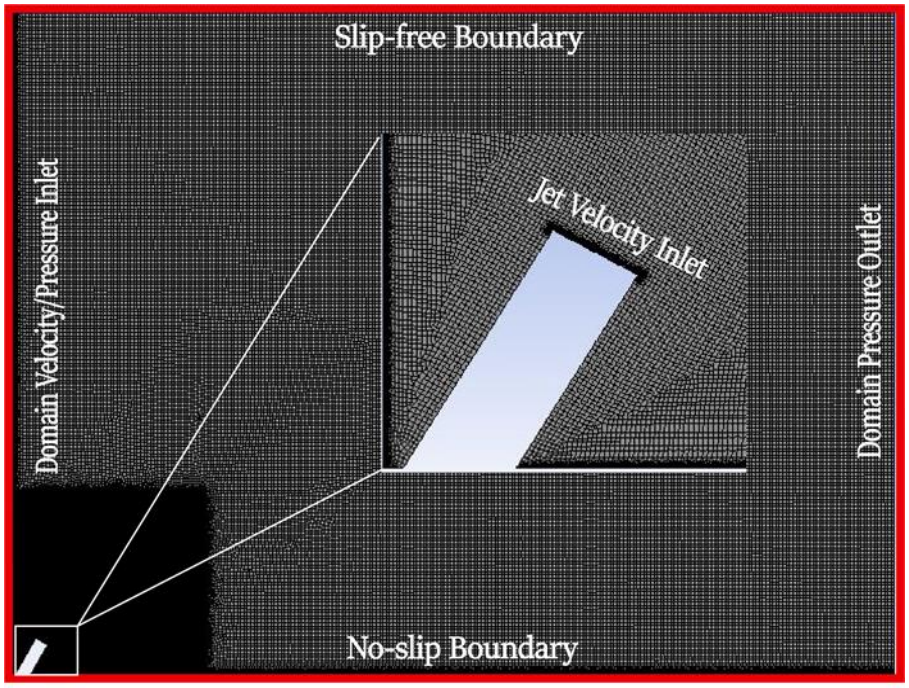

Fig. 2. Model geometry and the refined mesh grid

Results and Discussion

In this section, the results of the SST *k*-ω model are presented and compared with experimental data of Cipollina et al. [51], Kikkert et al. [52], Roberts et al. [38,40], Papakonstantis et al. [53,54], Abessi et al. [41], and numerical results of JETLAG, UM3, and CORJET by Palomar et al. [27]. The accuracy of all four models is quantitatively evaluated using error statistics.

Maximum Rise Height

The maximum rise height was calculated in four Froude numbers (F=10, 20, 30, and 40) for stagnant, and in F=20 and five current velocities for dynamic ambient. The data were normalized by dividing to the maximum value of Z_m ($Z_{m,max}$) reported by Cipollina et al. [51] for stagnant and calculated by CFD in the dynamic ambient.

Fig. 3 compares the results of maximum rise height (Z_m) provided by this study, three integral models and experimental data in stagnant ambient. All models follow the trend of experimental data very well; nevertheless, in all cases, integral models have underestimated the maximum rise height. Their deviation from the experimental data might be due to their instabilities on the edge of the jet when initial momentum counterbalances the buoyancy force [52,55].

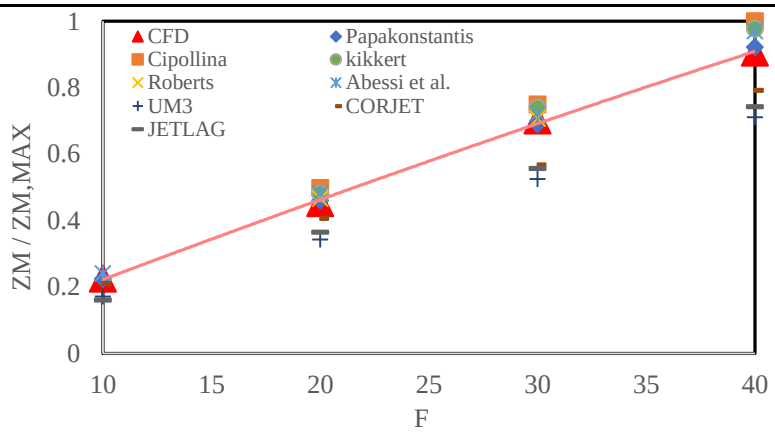

Fig. 3. Comparison of normalized maximum rise height in the stagnant ambient

As shown in this figure and Fig. 4, comparing the experimental data reported by Abessi et al. [39] with numerical results reveals that the CFD model has provided more accurate and reliable results. It seems that apart from using more logical hypotheses and more precise solvers, high-resolution refined meshes near the critical points has led to higher accuracy of the CFD model as compared with other models and data [56].

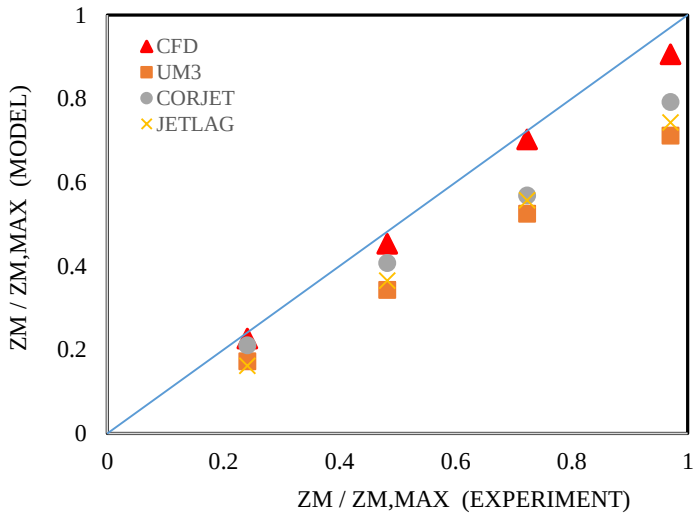

Fig. 4. Comparison of experimental data with the model prediction for stagnant ambient

Fig. 5 shows the results of maximum rise height (Z_m) provided by this study, three integral models by Palomar et al. [27] and experimental data by Roberts et al. [38] in dynamic ambient. As shown in this figure, the CFD model predicts the maximum rise height in the dynamic ambient better than any tools [40]. It is worthwhile to mention, at high ambient current velocity ($U_rF=1.87$), the model precision decreases, as the discrepancy rises to around 20% whereas it is less than 10% in lower U_rF. This can be attributed to the fact that using a 2D RANS model leads to a decrease in the number of equations and this can affect the modeling precision. However, CFD model still predicts experimental data with less deviation as compared to integral models.

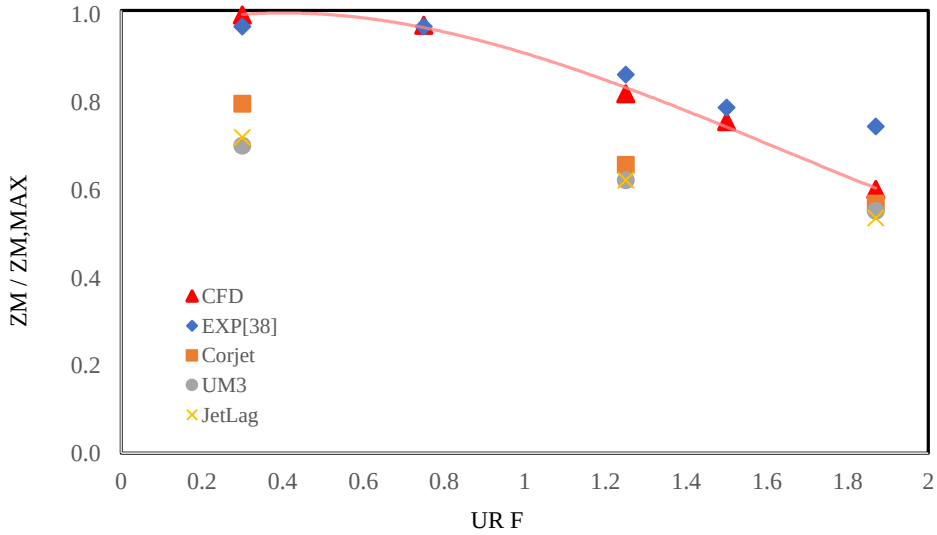

Fig. 5. Comparison of various models of normalized maximum rise height in the dynamic ambient

Impact Point Dilution

The impact point dilution (S_i) was calculated through the following equation for stagnant and dynamic ambient.

$$S_i = \frac{\rho_0 - \rho_a}{\rho_i - \rho_a} \tag{16}$$

The results are then normalized by the maximum impact point dilution ($S_{i,max}$) reported by Kikkert et al. [52] in F=40 for stagnant ambient and by Palomar et al. [27] for dynamic ambient. Fig. 6 compares predicted the impact point dilution with Froude number with experimental data.

It is notable that commercial packages produced approximately the same results, and these are all *underestimated* the experimental data. However, CFD showed less deviation and better agreement with experimental data. Parity plot shown in Fig. 7, compares the modeling results with experimental data reported by Papakonstantis et al. [50]. It appears that more satisfactory performance of CFD in modeling the dilution pattern is attributed to the key role played by the turbulence model. While, integral models employ simple semi-empirical turbulence models, which may be considered as the main reason of underestimations by these models in the prediction of the dilution pattern [13].

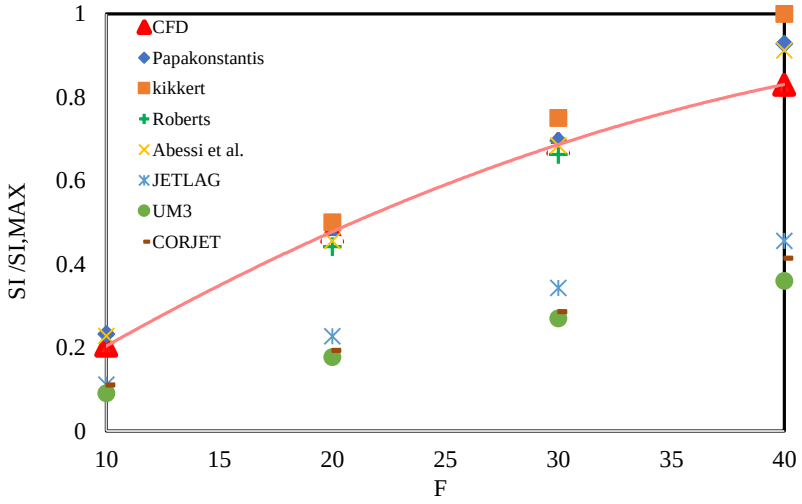

Fig. 6. Comparison of normalized impact point dilution in the stagnant ambient

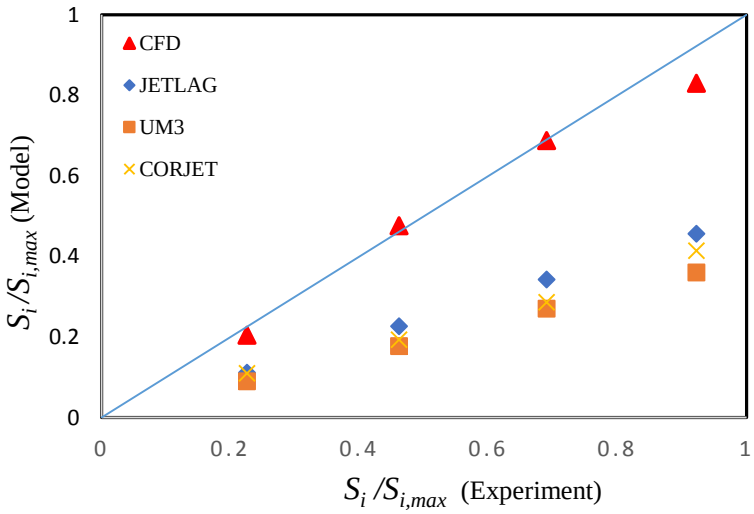

Fig. 7. Comparison of experimental data with model prediction at stagnant ambient

Fig. 8 compares the predicted impact point dilution by integral and CFD models with experimental data reported by Roberts et al. [38] at dynamic ambient. As shown in this figure, the CFD model simulated the dynamic ambient more accurately rather than stagnant ambient in terms of the impact point dilution only. From the results, it is understandable that modeling tools followed the experimental trend closely and the dilution is increased with the ambient current speed. It is important to mention that CORJET produces reliable results for impact point dilution especially at higher U_rF possibly due to its entrainment model; nevertheless, CFD is still well applicable to simulate dilution pattern in dynamic ambient.

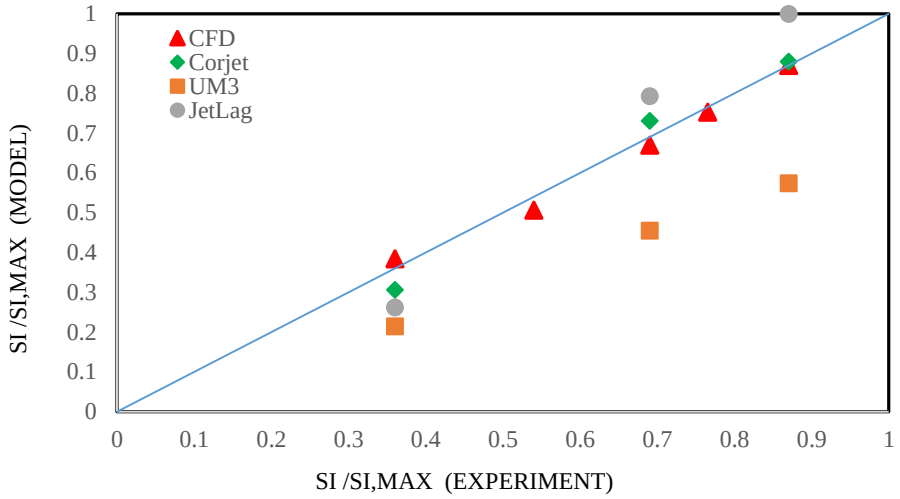

Fig. 8. Comparison of experimental data with model prediction at dynamic ambient

Error Statistics

To statistically compare the performance of CFD with integral models, the following expressions for BIAS, Scatter Index (SI) and correlation coefficient (CC) are used:

$$BIAS = \sum_{j=1}^{N} \frac{1}{N} \left(Y_j - X_j\right) \tag{17}$$

$$SI = \frac{\sqrt{(1/N) \sum_{j=1}^{N} \left(Y_j - X_j\right)^2}}{\bar{X}} \tag{18}$$

$$CC = \frac{\sum_{i=1}^{N} \left(X_j - \bar{X}\right)\left(Y_j - \bar{Y}\right)}{\sqrt{\sum_{j=1}^{N} \left(X_j - \bar{X}\right)^2 \sum_{j=1}^{N} \left(Y_j - \bar{Y}\right)^2}} \tag{19}$$

Where X_j are the experimental values, Y_j are calculated figures, N is the number of observations, $\bar{X}$ is the mean value of the experimental data. $\bar{Y}$ is the mean value of the model results. The statistical errors of maximum rise height and impact point dilution in stagnant and dynamic ambient are presented in Tables 4 and 5.

Table 4. BIAS, Scatter Index and Correlation Coefficient in the stagnant ambient

Error Statistics	Parameter	CFD	CORJET	JETLAG	UM3
BIAS	Z_m	0.005	-0.083	-0.128	-0.147
	S_l	-0.040	-0.531	-0.481	-0.572
Scatter Index	Z_m	0.023	0.165	0.218	0.260
	S_l	0.076	0.577	0.523	0.622
Correlation Coefficient	Z_m	0.999	0.999	0.999	0.999
	S_l	0.966	-0.993	0.837	0.996

Table 5. BIAS, Scatter Index and Correlation Coefficient in the Dynamic Ambient

Error Statistics	Parameter	CFD	CORJET	JETLAG	UM3
BIAS	Z_m	-0.050	-0.161	-0.209	-0.210
	S_l	0.001	-0.001	0.045	-0.225
Scatter Index	Z_m	0.103	0.194	0.254	0.257
	S_l	0.028	0.062	0.174	0.365
Correlation Coefficient	Z_m	0.976	0.977	0.953	0.952
	S_l	0.998	0.995	0.996	0.999

As seen in these tables, the CFD model performs better in the stagnant ambient than dynamic ambient in terms of jet maximum rise height prediction. However, error statistics, reported in these table for CFD model, show the higher accuracy of the CFD model in predicting the impact point dilution in dynamic as compared with stagnant ambient. Additionally, in consistent with findings reported in Fig. 8, statistical analyses of these tables also showed that the CFD performs quite better as compared with integral models.

Impact Point Location

Impact point locations, as calculated by Palomar et al. [27], were just limited to three averaged values in the stagnant ambient. In this study, the predicted average impact distances and their discrepancy from experimental data are reported in Table 6.

Table 6. Average Impact Point Location Calculated by CFD, CORJET, JETLAG, and UM3

Tool	CFD	CORJET	JETLAG	UM3
X_i/dF	2.85	2.22	2.33	1.97
Deviation (%)	11.7	12.9	8.6	22.7

The table shows that the performance of these models in predicting the impact point location is acceptable comparing with the experimental deviations of ~26% reported by Palomar et al. [27] and as a result, it seems that there is no need to focus on this part to make improvement in Modeling.

Comparison of 3D and Modified 2D Model

In this section, the results of the modified 2D model are compared with a three-dimensional model proposed by Baum et al. [5] and the deviation of both models from experimental data by Papakonstantis et al. [53,54] and Roberts et al. [38] are reported (Table 7). Using a 3D CFD model and the SST k-ω turbulence scheme, Baum et al. [5] modeled the discharge of brine from 60° single-port jets in stagnant and dynamic ambient.

Table 7. Comparison of 3D and Modified 2D Model

Ambient	Parameter	Exp. Data (Reference)	3D Model (Deviation)	Modified 2D Model (Deviation)
Stagnant (U_rF=0)	Z_m/dF	2.14 ([52])	2 (7%)	2.26 (5.3%)
	S_i/F	1.68 ([51])	0.95 (76.8%)	1.8 (6.6%)
Dynamic (U_rF=1.5)	Z_m/dF	1.8 ([38])	1.75 (2.9%)	1.725 (4.3%)
	S_i/F	2.6 ([38])	2.9 (10.3%)	2.51 (3.6%)

Comparing the data in Table 7, it seems that in most cases the results of the 2D model proposed in this study were close to the three-dimensional model by Baum et al. [5]. However, using mass transfer mechanism made a great contribution in predicting impact dilution in the stagnant ambient according to deviation values. Minor improvements over the 3D model in predicting other parameters can be due to the quality of the mesh. In general, not only does a two-dimensional model lead to a significant reduction in computational costs, but also it provides accurate results, in some cases more accurate than 3D models, by applying proper details to it.

Conclusion

In this paper, simulations were conducted to investigate the accuracy of modified CFD model in predicting dense jets behavior in stagnant and dynamic ambient. The qualitative and quantitative comparison among CFD and integral models with experimental data were made through parity plots and statistical analyses. In the stagnant ambient, the maximum rise height predictions reveal that the models followed the experimental trend. However, CFD provides far promising results, especially in higher Froude numbers, where integral models

underestimated the maximum rise height as well as the impact point dilution. In dynamic ambient, although the precision of the CFD model on the maximum rise height was lower, its performance in calculating the impact point dilution was considerably higher as compared with stagnant ambient. This is also valid for integral models, particularly in high ambient current speeds, where the CORJET model agreed quite well with the experimental data. Therefore, this study showed that the modified CFD model precisely predicted experimental data better than integral models. Moreover, comparing the results of the 2D model with a 3D model propsed in the literature revealed that 2D models can predict dense jets behavior accurately while they are more computationally efficient. The results of this study can be used to extend the application of CFD modeling in the prediction of the performance of inclined jets for brine dilutions.

References

[1] Lykkebo Petersen, K., Heck, N., G Reguero, B., Potts, D., Hovagimian, A., Paytan, A.: Biological and physical effects of brine discharge from the Carlsbad desalination plant and implications for future desalination plant constructions. Water 11(2), 208 (2019). https://doi.org/10.3390/w11020208

[2] Baum, M.J., Albert, S., Grinham, A., Gibbes, B.: Spatiotemporal influences of open-coastal forcing dynamics on a dense multiport diffuser outfall. Journal of Hydraulic Engineering 145(10), 05019004 (2019). https://doi.org/10.1061/(ASCE)HY.1943-7900.0001622

[3] Roberts, D.A., Johnston, E.L., Knott, N.A.: Impacts of desalination plant discharges on the marine environment: A critical review of published studies. Water research 44(18), 5117-5128 (2010). https://doi.org/10.1016/j.watres.2010.04.036

[4] Greenlee, L.F., Lawler, D.F., Freeman, B.D., Marrot, B., Moulin, P.: Reverse osmosis desalination: water sources, technology, and today's challenges. Water research 43(9), 2317-2348 (2009). https://doi.org/10.1016/j.watres.2009.03.010

[5] Baum, M., Gibbes, B.: Improved understanding of dense jet dynamics to guide management of desalination outfalls. In: Vol. 1 of Proc., MODSIM2017, 22nd Int. Congress on Modelling and Simulation Society of Australia and New Zealand, edited by G. Syme, D. Hatton MacDonald, B. Fulton, and J. Piantadosi, Hobart 2017, pp. 1711-1717. http://dx.doi.org/10.36334/modsim.2017.L11.baum

[6] Rezaei-DashtArzhandi, M., Sarrafzadeh, M., Goh, P., Lau, W., Ismail, A., Mohamed, M.: Development of novel thin film nanocomposite forward osmosis membranes containing halloysite/graphitic carbon nitride nanoparticles towards enhanced desalination performance. Desalination 447, 18-28 (2018). https://doi.org/10.1016/j.desal.2018.08.003

[7] Roy, A., Moulik, S., Kamesh, R., Mullick, A.: Modeling in Membranes and Membrane-Based Processes. Newark: John Wiley & Sons, Incorporated, 47-50 (2020). https://doi.org/10.1002/9781119536260

[8] Jones, E., Qadir, M., van Vliet, M.T., Smakhtin, V., Kang, S.-m.: The state of desalination and brine production: A global outlook. Science of the Total Environment 657, 1343-1356 (2019). https://doi.org/10.1016/j.scitotenv.2018.12.076

[9] Pramanik, B.K., Shu, L., Jegatheesan, V.: A review of the management and treatment of brine solutions. Environmental Science: Water Research & Technology 3(4), 625-658 (2017). https://doi.org/10.1039/c6ew00339g

[10] Stefanakis, A.I., Becker, J.A.: A review of emerging contaminants in water: classification, sources, and potential risks. In: Impact of Water Pollution on Human Health and Environmental Sustainability. pp. 55-80. IGI Global, (2016). https://doi.org/10.4018/978-1-4666-9559-7.ch003

[11] Frank, H., Fussmann, K.E., Rahav, E., Zeev, E.B.: Chronic effects of brine discharge form large-scale seawater reverse osmosis desalination facilities on benthic bacteria. Water research 151, 478-487 (2019). https://doi.org/10.1016/j.watres.2018.12.046

[12] Ibrahim, H.D., Eltahir, E.A.: Impact of Brine Discharge from Seawater Desalination Plants on Persian/Arabian Gulf Salinity. Journal of Environmental Engineering 145(12), 04019084 (2019). https://doi.org/10.1061/(asce)ee.1943-7870.0001604

[13] Gude, G.: Sustainable desalination handbook: plant selection, design and implementation. Butterworth-Heinemann, (2018). https://doi.org/10.1016/b978-0-12-809240-8.00001-0

[14] Panagopoulos, A., Haralambous, K.-J., Loizidou, M.: Desalination brine disposal methods and treatment technologies-A review. Science of the Total Environment 693, 133545 (2019). https://doi.org/10.1016/j.scitotenv.2019.07.351

[15] Yan, X., Mohammadian, A.: Numerical modeling of multiple inclined dense jets discharged from moderately spaced ports. Water 11(10), 2077 (2019). https://doi.org/10.3390/w11102077

[16] Zhang, S., Jiang, B., Law, A.W.-K., Zhao, B.: Large eddy simulations of 45 inclined dense jets. Environmental Fluid Mechanics 16(1), 101-121 (2016). https://doi.org/10.1007/s10652-015-9415-2

[17] Zeitoun, M., Reid, R., McHilhenny, W., Mitchell, T.: Model studies of outfall system for desalination plants. Research and Development Progress Rep. 804, Office of Saline Water, U.S Washington, DC: Dept. of Interior (1970). https://doi.org/10.4043/1370-ms

[18] Abessi, O., Roberts, P.J.: Effect of nozzle orientation on dense jets in stagnant environments. Journal of Hydraulic Engineering 141(8), 06015009 (2015). https://doi.org/10.1061/(asce)hy.1943-7900.0001032

[19] Abessi, O., Roberts, P.J.: Dense jet discharges in shallow water. Journal of Hydraulic Engineering 142(1), 04015033 (2016). https://doi.org/10.1061/(asce)hy.1943-7900.0001057

[20] Palomar, P., Lara, J., Losada, I., Rodrigo, M., Alvárez, A.: Near field brine discharge modelling part 1: Analysis of commercial tools. Desalination 290, 14-27 (2012). https://doi.org/10.1016/j.desal.2011.11.037

[21] Palomar, P., Losada, I.J.: Impacts of brine discharge on the marine environment. Modelling as a predictive tool. Desalination, trends and technologies 234 (2011). https://doi.org/10.5772/14880

[22] Sahlodin, A.M., Sotudeh-Gharebagh, R., Zhu, Y.: Modeling of dispersion near roadways based on the vehicle-induced turbulence concept. Atmospheric Environment 41(1), 92-102 (2007). https://doi.org/10.1016/j.atmosenv.2006.08.004

[23] Witlox, H.W., Stene, J., Harper, M., Nilsen, S.H.: Modelling of discharge and atmospheric dispersion for carbon dioxide releases including sensitivity analysis for wide range of scenarios. Energy Procedia 4, 2253-2260 (2011). https://doi.org/10.1016/j.egypro.2011.02.114

[24] Kwak, K.-H., Baik, J.-J.: A CFD modeling study of the impacts of NOx and VOC emissions on reactive pollutant dispersion in and above a street canyon. Atmospheric environment 46, 71-80 (2012). https://doi.org/10.1016/j.atmosenv.2011.10.024

[25] Gousseau, P., Blocken, B., Stathopoulos, T., Van Heijst, G.: CFD simulation of near-field pollutant dispersion on a high-resolution grid: a case study by LES and RANS for a building group in downtown Montreal. Atmospheric Environment 45(2), 428-438 (2011). https://doi.org/10.1016/j.atmosenv.2010.09.065

[26] Chow, M.M., Cardoso, S.S.S., Holford, J.M.: Dispersion of Pollutants Discharged into the Ocean: The Interaction of Small- and Large-scale Phenomena. Chemical Engineering Research and Design 82(6), 730-736 (2004). https://doi.org/10.1205/026387604774196019

[27] Palomar, P., Lara, J., Losada, I.: Near field brine discharge modeling part 2: Validation of commercial tools. Desalination 290, 28-42 (2012). https://doi.org/10.1016/j.desal.2011.10.021

[28] Vafeiadou, P., Papakonstantis, I., Christodoulou, G.: Numerical simulation of inclined negatively buoyant jets. In: The 9th international conference on environmental science and technology, September 2005, pp. 1-3 https://doi.org/10.1080/00221686.2010.537153

[29] Oliver, C., Davidson, M., Nokes, R.: k-ε Predictions of the initial mixing of desalination discharges. Environmental Fluid Mechanics 8(5-6), 617 (2008). https://doi.org/10.1007/s10652-008-9108-1

[30] Robinson, D., Wood, M., Piggott, M., Gorman, G.: CFD modelling of marine discharge mixing and dispersion. Journal of Applied Water Engineering and Research 4(2), 152-162 (2016). https://doi.org/10.1080/23249676.2015.1105157
[31] Gildeh, H.K., Mohammadian, A., Nistor, I., Qiblawey, H.: Numerical modeling of 30 and 45◦ inclined dense turbulent jets in stationary ambient. Environmental Fluid Mechanics 15(3), 537-562 (2015). https://doi.org/10.1007/s10652-014-9372-1
[32] Zhang, S., Law, A.W.-K., Jiang, M.: Large eddy simulations of 45 and 60 inclined dense jets with bottom impact. Journal of hydro-environment research 15, 54-66 (2017). https://doi.org/10.1016/j.jher.2017.02.001
[33] Jiang, M., Law, A.W.-K., Lai, A.C.: Turbulence characteristics of 45 inclined dense jets. Environmental Fluid Mechanics 19(1), 27-54 (2019). https://doi.org/10.1007/s10652-018-9614-8
[34] Ardalan, H., Vafaei, F.: CFD and Experimental Study of 45 Inclined Thermal-Saline Reversible Buoyant Jets in Stationary Ambient. Environmental Processes 6(1), 219-239 (2019). https://doi.org/10.1007/s40710-019-00356-z
[35] Baum, M.J., Gibbes, B.: Field-Scale Numerical Modeling of a Dense Multiport Diffuser Outfall in Crossflow. Journal of Hydraulic Engineering 146(1), 05019006 (2020). https://doi.org/10.1061/(asce)hy.1943-7900.0001635
[36] Al-Sanea, S., Orfi, J., Najib, A.: Numerical study of flow, temperature, and salinity distributions of a brine discharge problem. Desalination and Water Treatment 55(12), 3218-3230 (2015). https://doi.org/10.1080/19443994.2014.940658
[37] Ardalan, H., Vafaei, F.: Hydrodynamic classification of submerged Thermal-Saline Inclined Single-Port discharges. Marine Pollution Bulletin 130, 299-306 (2018). https://doi.org/10.1016/j.marpolbul.2018.03.052
[38] Roberts, P.J., Ferrier, A., Daviero, G.: Mixing in inclined dense jets. Journal of Hydraulic Engineering 123(8), 693-699 (1997). https://doi.org/10.1061/(asce)0733-9429(1997)123:8(693)
[39] List, E., Koh, R.C., Imberger, J.: Mixing in inland and coastal waters. Academic Press, (1979). https://doi.org/10.1016/c2009-0-22051-4
[40] Roberts, P.J., Toms, G.: Inclined dense jets in flowing current. Journal of Hydraulic Engineering 113(3), 323-340 (1987). https://doi.org/10.1061/(asce)0733-9429(1987)113:3(323)
[41] Abessi, O., Roberts, P.J.: Multiport diffusers for dense discharges. Journal of Hydraulic Engineering 140(8), 04014032 (2014). https://doi.org/10.1061/(asce)hy.1943-7900.0000882
[42] Abessi, O., Roberts, P.J.: Multiport diffusers for dense discharge in flowing ambient water. Journal of Hydraulic Engineering 143(6), 04017003 (2017). https://doi.org/10.1061/(asce)hy.1943-7900.0001279
[43] Manninen, M., Taivassalo, V., Kallio, S.: On the mixture model for multiphase flow. In. Technical Research Centre of Finland Finland, (1996)
[44] Xue, W., Huai, W., Qian, Z., Yang, Z., Zeng, Y.: Numerical simulation of initial mixing of marine wastewater discharge from multiport diffusers. Engineering Computations 31(7), 1379-1400 (2014). https://doi.org/10.1108/ec-06-2013-0148
[45] Schiller, L.: A drag coefficient correlation. Zeit. Ver. Deutsch. Ing. 77, 318-320 (1933).
[46] Morsi, S., Alexander, A.: An investigation of particle trajectories in two-phase flow systems. Journal of Fluid mechanics 55(2), 193-208 (1972). https://doi.org/10.1017/s0022112072001806
[47] Fluent, A.: 18.1, Theory Guide, Ansys. In. Inc, (2017)
[48] Seil, G., Zhang, Q.: CFD modeling of desalination plant brine discharge systems. J. Aust. Water Assoc 37(6), 79-83 (2010).
[49] Menter, F.R.: Two-equation eddy-viscosity turbulence models for engineering applications. AIAA journal 32(8), 1598-1605 (1994). https://doi.org/10.2514/3.12149

[50] Patankar, S.V.: Numerical heat transfer and fluid flow, Hemisphere Publ. Corp., New York 58 (1980). https://doi.org/10.1002/cite.330530323

[51] Cipollina, A., Brucato, A., Grisafi, F., Nicosia, S.: Bench-scale investigation of inclined dense jets. Journal of Hydraulic Engineering 131(11), 1017-1022 (2005). https://doi.org/10.1061/(asce)0733-9429(2005)131:11(1017)

[52] Kikkert, G., Davidson, M., Nokes, R.: Inclined negatively buoyant discharges. Journal of Hydraulic Engineering 133(5), 545-554 (2007). https://doi.org/10.1061/(asce)0733-9429(2007)133:5(545)

[53] Papakonstantis, I.G., Christodoulou, G.C., Papanicolaou, P.N.: Inclined negatively buoyant jets 2: concentration measurements. Journal of Hydraulic Research 49(1), 13-22 (2011). https://doi.org/10.1080/00221686.2010.542617

[54] Papakonstantis, I.G., Christodoulou, G.C., Papanicolaou, P.N.: Inclined negatively buoyant jets 1: geometrical characteristics. Journal of Hydraulic Research 49(1), 3-12 (2011). https://doi.org/10.1080/00221686.2010.537153

[55] Shao, D., Law, A.: Integral modelling of horizontal buoyant jets with asymmetrical cross sections. In: Proceedings of the 7th International Symposium on Environmental Hydraulics 2014

[56] Dissanayake, A.L., Gros, J., Socolofsky, S.A.: Integral models for bubble, droplet, and multiphase plume dynamics in stratification and crossflow. Environmental Fluid Mechanics 18(5), 1167-1202 (2018). https://doi.org/10.1007/s10652-018-9591-y

How to cite: Moshiri-Tabrizi I, Sarrafzadeh M-H, Sotudeh-Gharebagh R. 2D-CFD Analysis of Diffusers Used to Discharge Brine into Water Bodies. Journal of Chemical and Petroleum Engineering 2023; 57(2): 303-319.